Progress In Electromagnetics Research M, Vol. 49, 181–193, 2016

Calculation of Force between Two Ring Magnets Using Adaptive Monte Carlo Technique with Experimental Verification

Tapan Santra[1, *], Debabrata Roy[1], and Sotoshi Yamada[2]

Abstract—This paper represents a new simple technique to calculate force between two ring magnets using adaptive Monte Carlo integration technique. Elementary magnetic force is calculated by discretizing the pole faces of the passive magnets into tiny surfaces. To obtain the resultant force, this elementary force equation is integrated over the dimensions of the ring magnets which incur a multidimensional integration with complicated integral function. This multidimensional integration is solved using adaptive Monte Carlo technique considering singularity treatment and importance sampling. This method is advantageous over existing analytical or quasi analytical methods regarding singularity treatment and computational burden. It is more flexible, especially for using in digital computer. The result of the proposed technique is verified with finite element method and also validated by laboratory experiment. It is observed that the proposed result matches very well with the practical test result, particularly if self demagnetization is considered. So taking into account of simplicity, less computational burden and usefulness, the proposed method may be an alternative choice for magnetic force calculation.

1. INTRODUCTION

Magnet configuration consists of two passive ring magnets and is customarily used in flywheel energy storage [1], turbo molecular pump, conveyor system [2], turbo machines, micro mass measurement [3], magnetic bearing [4] and space application. To develop the mathematical model of these devices we need to calculate force between two ring magnets. This developed model finds application in the design of magnetic devices, performance analysis, control and dimension optimization. So there are some aspects in force calculation, which should be precise, simple and have less computational burden. Some analytical or quasi-analytical methods have already been developed by Lang [5], Jiang et al. [6], Ravaud et al. [7–9] and Bekinal et al. [10] for modelling the magnetic field. Lijesh and Hirani [11] developed some analytical equations for design and optimization of axially polarized radial passive magnetic bearing and performed some wonderful case studies. But these methods do not handle singularity of the integral over the integration domain satisfactorily. Most of the existing methods require some analytical transformation or preprocessing for singularity treatment, but in this method singularity is taken care only by avoiding samples in the singular zone by writing a simple computer code. Moreover, some existing methods involve elliptic integral which is tedious to solve analytically, and computation burden is also high. So these methods are not suitable for dimension optimization, design and control of the magnetic system. In this paper, a 3D model of magnetic force is developed using surface charge density method. The expression of this magnetic force involves a four-dimensional integration with complicated integral, which is solved by Monte Carlo Integration [12] technique. The integral may involve singularity

Received 21 May 2016, Accepted 16 July 2016, Scheduled 30 August 2016

* Corresponding author: Tapan Santra (tapan_santra98@yahoo.co.in).

[1] Electrical Engineering Department, Indian Institute of Engineering Science & Technology, Shibpur, Howrah-711103, WB, India.

[2] Division of Biological Measurement and Application, Institute of Nature and Environmental Technology (K-INET), Kanazawa University, Japan.

and irregular distribution of integral values in the domain. We investigate the singularity of the integral over the domain. In our problem, the integrand does not contain any singularity due to some practical constraints imposed, but there are some large peaks in the domain which gives the principal contribution to the integral. Due to these peaks, there is some error in the estimation.

The flat distribution of sample points invites error in the calculation unless numbers of samples are very large. On the contrary, if number of samples is very large, computational cost will be high. Due to this uneven distribution of integrand, we consider adaptive distribution of sample points [13–15] so that more samples are selected near peak and few samples in the flat region in the domain. Thus integration error is minimized by reducing the variance. This is called Adaptive Monte Carlo integration (AMC). The result of the proposed AMC technique is verified with finite element method (FEM, MAXWELL) and also validated by laboratory experiment. The results of these three methods, thus obtained, are found to be in close agreement with each other.

2. CALCULATION OF FORCE BETWEEN TWO RING MAGNETS

2.1. Configuration and Dimensions of the Magnetic System

Figure 1 shows that the magnetic configuration consists of two concentric ring magnets with axial polarization. It is a very popular configuration due to its simplicity and application perspective in energy storing flywheel, micro mass measurement, magnetic bearing and space application. Generally, the outer magnet is attached with the static frame, and the inner magnet is free to move along different axes. The dimensions of the system are shown in Figure 1. R_1, R_2 are the inner and outer radii of inner magnet. R_3, R_4 are the inner and outer radii of outer magnet. L is the thickness of the magnets. Objective of this work is to efficiently calculate the 3D force acting between these two magnets using AMC integration technique. Pole faces of the magnets are discretized into small elementary surfaces, and interaction between these elementary surfaces gives elementary magnetic force. Integration of this elementary force over the magnet dimensions gives the resultant force between the magnets.

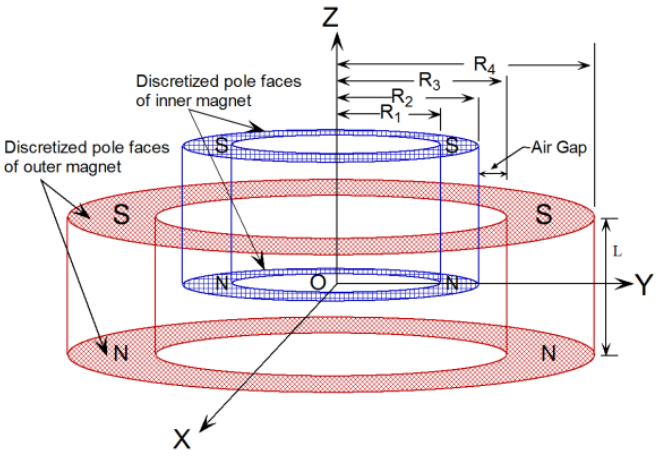

Figure 1. Configuration of the passive magnets with dimensions and discretised pole faces.

2.2. Calculation of the Magnetic Force

To derive the analytical expression of force between two passive magnets, different methods are available. There are mainly three existing methods, Dipole method, Amperian current model and Columbian surface charge density method. In our work, the relative magnet dimensions are more than the air gap dimension, so dipole method does not give accurate result. We apply simple Columbian surface charge density method. According to this method, it is assumed that magnetic charges are distributed on the faces of magnetic poles Q, R, S and T as shown in Figure 2(a). Magnetic forces are generated due to the interaction between the charges of these magnet faces. Let the inner magnet be displaced from

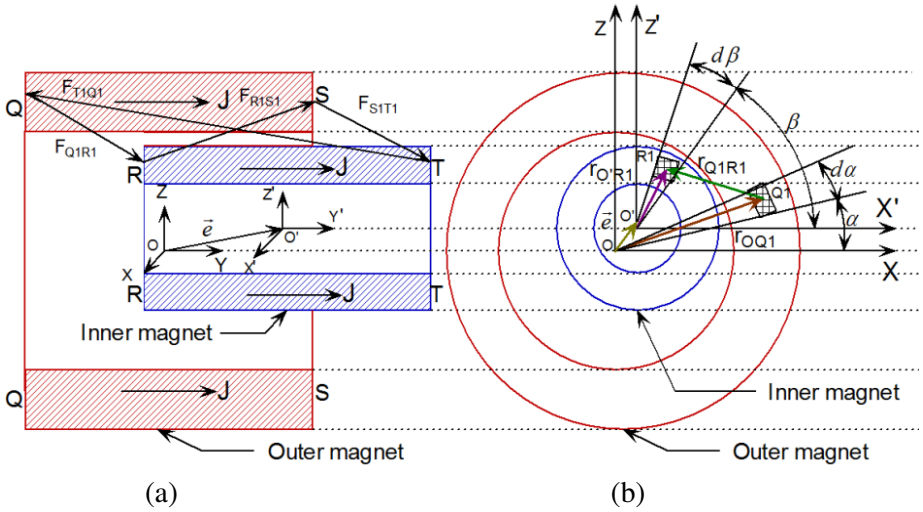

Figure 2. (a) Forces acting on inner magnet after a translation e in Y-Z plane. (b) Elementary force between two tiny magnetic surfaces on outer and inner magnets in Z-X plane.

the nominal position $O(0,0,0)$ to $O'(x,y,z)$ due to a translation $\vec{e} = x\hat{i} + y\hat{j} + z\hat{k}$ in 3D plane XYZ, where $\hat{i}$, $\hat{j}$ and $\hat{k}$ are the unit vectors along X, Y and Z axes, respectively. The pole faces Q, R, S and T are discretized into a number of small elementary surfaces. Let $Q1$, $R1$, $S1$, and $T1$ be one of such elements. J is the polarization of magnets. So there are magnetic forces of attraction ($\vec{F}_{T1Q1}$ and $\vec{F}_{R1S1}$) between $T1$-$Q1$ and $R1$-$S1$, respectively. There are repulsive forces ($\vec{F}_{Q1R1}$ and $\vec{F}_{S1T1}$) acting between $Q1$-$R1$ and $S1$-$T1$, respectively. Figure 2(b) shows the distance vector between elements $Q1$ and $R1$ in X-Z plane. The elementary magnetic force between the elementary surfaces $Q1$ and $R1$ is given by Coulomb law in Eq. (1).

$$d\vec{F}_{Q1R1} = \frac{\mu_0 q_{Q1} q_{R1}}{4\pi R^3_{Q1R1}} \vec{r}_{Q1R1} \tag{1}$$

where, q_{Q1} and q_{R1} are the fictitious charge of elementary magnetic surfaces $Q1$ on outer magnet and $R1$ on inner magnet, respectively. $\vec{r}_{Q1R1}$ is the distance vector between elements $Q1$ and $R1$. Now q_{Q1} and q_{R1} are expressed in terms of surface charge density σ and elementary surface areas dS_{Q1} and dS_{R1} as shown in Eq. (2)

$$q_{Q1} = \sigma_{Q1} dS_{Q1}, \quad q_{R1} = \sigma_{R1} dS_{R1} \tag{2}$$

Surface areas of two elements $Q1$ and $R1$ are expressed in terms of radius vectors r_{OQ1}, $r_{O'R1}$ and incremental angle variables $d\alpha$, $d\beta$ about outer magnet centre O and inner magnet centre O' respectively as shown in Figure 2(b).

$$dS_{Q1} = r_{OQ1} d\alpha dr_{OQ1}, \quad dS_{R1} = r_{O'R1} d\beta dr_{O'R1} \tag{3}$$

Now for a linear isotopic homogeneous magnetic material, magnetic induction B is given in terms of magnetization M and magnetic field H by Eq. (4)

$$B = \mu_0 (H + M) \tag{4}$$

$$M = (\mu_r - 1)(H + M_r) \tag{5}$$

For a rare earth material $\mu_r \approx 1$, so from Eq. (5)

$$M = M_r \tag{6}$$

When $H = 0$, using Eqs. (4) and (6)

$$B_r = \mu_0 M_r \tag{7}$$

If it is assumed that the material is uniformly magnetized, then

$$M_r = \sigma \tag{8}$$

So the surface charge density σ can be expressed in terms of magnetic induction B_r as shown in Eq. (4).

$$\sigma = \frac{B_r}{\mu_0} \tag{9}$$

To get accurate B_r value, self demagnetizing effect of the magnet is to be considered. Metal alloy is not going to be magnetized. Permanent magnet always has a tendency to reduce the energetic state from high energy state by demagnetization. The geometry of the magnet greatly influences the demagnetizing process. First the permeance coefficient P_c is calculated for the ring magnets. Using method stated in [16], P_c at open circuit condition is given for different geometries in Figure 3(a). For the given geometry of ring magnet given in Table 1, calculated P_c of one magnet is 1.7. Corresponding reduction in magnetic induction B_r is observed in Figure 3(b). It is observed that almost 5% reduction occurs. Let the corrected value of magnetic induction be B_{rc}.

Table 1. Parameters of the magnetic system.

Material of magnets	NdFeB
Coercivity (H_{ci})	$1.3 * 10^6$ A/m
Flux density (B)	1.27 T
Outer radius of outer magnet (R_4)	0.030 m
Inner radius of outer magnet (R_3)	0.020 m
Outer radius of inner magnet (R_2)	0.018 m
Inner radius of inner magnet (R_1)	0.010 m
Thickness of magnets (L)	0.010 m

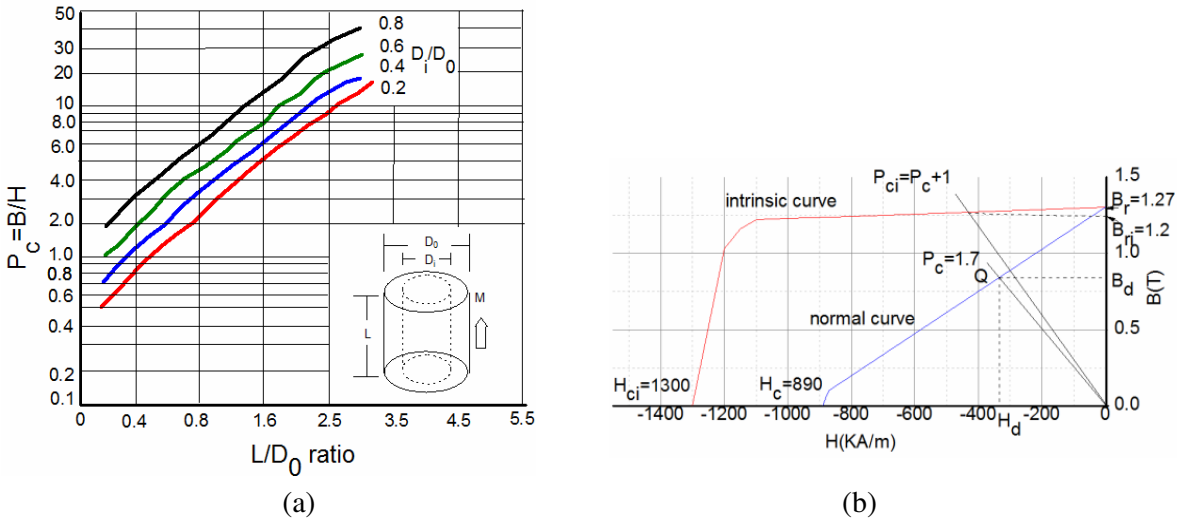

Figure 3. (a) Permeance coefficient of ring magnet for different geometries with axial polarization. (b) Calculation of corrected magnetic induction considering self demagnetizing.

Using Eqs. (1), (2), (3) and (9), we get the elementary force expression (10)

$$d\vec{F}_{Q1R1} = \frac{B_{rc}^2 r_{OQ1} r_{O'R1} dr_{OQ1} dr_{O'R1} d\alpha d\beta}{4\pi\mu_0 r_{Q1R1}^3} \vec{r}_{Q1R1} \tag{10}$$

Distances of elements $Q1$ and $R1$ about rotor magnet centre O' are given by Eqs. (11) and (12),

respectively, as shown in Figure 2(b).

$$\vec{r}_{O'Q1} = X_{Q1}\hat{i} + Y_{Q1}\hat{j} + Z_{Q1}\hat{k} = (r_{OQ1}\cos\alpha - x)\,\hat{i} + (r_{OQ1}\sin\alpha - y)\,\hat{j} + \left(-z - \frac{H}{2}\right)\hat{k} \quad (11)$$

$$\vec{r}_{O'R1} = X_{R1}\hat{i} + Y_{R1}\hat{j} + Z_{R1}\hat{k} = (r_{O'R1}\cos\beta)\,\hat{i} + (r_{O'R1}\sin\beta)\,\hat{j} + \left(-\frac{H}{2}\right)\hat{k} \quad (12)$$

Using Eqs. (11) and (12), we obtain the distance vector between elements $Q1$ and $R1$ as per Eq. (13).

$$\begin{aligned}\vec{r}_{Q1R1} &= \vec{r}_{O'Q1} - \vec{r}_{O'R1} = (X_{Q1} - X_{R1})\,\hat{i} + (Y_{Q1} - Y_{R1})\,\hat{j} + (Z_{Q1} - Z_{R1})\,\hat{k} \\ &= (r_{OQ1}\cos\alpha - x - r_{O'R1}\cos\beta)\,\hat{i} + (r_{OQ1}\sin\alpha - y - r_{O'R1}\sin\beta)\,\hat{j} + (-z)\hat{k} \end{aligned} \quad (13)$$

Using Eq. (13) in Eq. (10), elementary force between charged magnetic elements $Q1$ and $R1$ is given by Eq. (14)

$$d\vec{F}_{Q1R1} = \frac{B_{rc}^2 r_{OQ1} r_{O'R1}}{4\pi\mu_0 (R_{Q1R1})^3} \begin{bmatrix} (r_{OQ1}\cos\alpha - x - r_{O'R1}\cos\beta)\,\hat{i} \\ +\,(r_{OQ1}\sin\alpha - y - r_{O'R1}\sin\beta)\,\hat{j} \\ +(-z)\hat{k} \end{bmatrix} dr_{OQ1} dr_{O'R1} d\alpha d\beta \quad (14)$$

where $R_{Q1R1} = \sqrt{(r_{OQ1}\cos\alpha - x - r_{O'R1}\cos\beta)^2 + (r_{OQ1}\sin\alpha - y - r_{O'R1}\sin\beta)^2 + (-z)^2}$.

To calculate total magnetic force between outer magnet pole face Q and inner magnet pole face R, all the tiny discretized elementary magnetic surfaces on Q and R should be considered. So the resultant force between Q and R is the integration of the elementary force given in Eq. (14) over the dimensions of the magnets, and this is given by Eq. (15).

$$\vec{F}_{QR} = \frac{B_{rc}^2}{4\pi\mu_0} \int_{r_{OQ1}=R_1}^{R_2} \int_{r_{O'R1}=R_3}^{R_4} \int_{\alpha=0}^{2\pi} \int_{\beta=0}^{2\pi} f\,(r_{OQ1}, r_{O'R1}, \alpha, \beta)\, dr_{OQ1} dr_{O'R1} d\alpha d\beta \quad (15)$$

where

$$\begin{aligned} f\,(r_{OQ1}, r_{O'R1}, \alpha, \beta) &= \frac{r_{OQ1} r_{O'R1}}{(R_{Q1R1})^3} \Big[(r_{OQ1}\cos\alpha - x - r_{O'R1}\cos\beta)\,\hat{i} \\ &\quad + (r_{OQ1}\sin\alpha - y - r_{O'R1}\sin\beta)\,\hat{j} + (-z)\hat{k} \Big] \end{aligned}$$

Solution of Eq. (15) gives the force between magnet surfaces Q and R as given by Eq. (16).

$$\vec{F}_{QR} = F_{QRx}\hat{i} + F_{QRy}\hat{j} + F_{QRz}\hat{k} \quad (16)$$

In a similar manner, described in Eqs. (1)–(16), magnetic forces between other surfaces T-Q, R-S and S-T are calculated, and resultant force between outer and inner magnets is represented in Eq. (17).

$$\begin{aligned} \vec{F}_{\text{total}} &= (F_{QRX} + F_{TQX} + F_{RSX} + F_{STX})\,\hat{i} + (F_{QRY} + F_{TQY} + F_{RSY} + F_{STY})\,\hat{j} \\ &\quad + (F_{QRZ} + F_{TQZ} + F_{RSZ} + F_{STZ})\,\hat{k} = F_X\hat{i} + F_Y\hat{j} + F_Z\hat{k} \end{aligned} \quad (17)$$

Analytical expression (15) is a function of four variables r_{OQ1}, $r_{O'R1}$, α, β, which is very complicated to visualize. The dimensions of the integrand are reduced to two by a simple transformation $\nabla r = r_{OQ1} - r_{O'R1}$ and $\nabla\theta = \alpha - \beta$.

Total axial force for a displacement $x = 0\,\text{m}$, $y = 0\,\text{m}$, $z = 5 \times 10^{-3}\,\text{m}$ is computed using Eq. (17) and shown in Figure 4(a). There are three peaks as $\nabla r \to 0$, $\nabla\theta \to 0$ or $\nabla\theta \to 2\pi$. This is expected as the repulsive force between any two elementary magnet surfaces on inner and outer magnets is high when distance between them is less. Other portions of the Figure 4(a) is flat and of less important for integration. A surface fitting is carried out by Gaussian function using Levenberg Marquardt iteration algorithm, and the expression of fitted function is given by Eq. (18). The parameters of the fitted function are shown in Table 2, and a contour plot of the corresponding function is shown in Figure 4(b).

$$t = t_0 + A * \exp\left(-0.5 * \left(\frac{r - r_c}{w_1}\right)^2 - 0.5 * \left(\frac{s - s_c}{w_2}\right)^2\right) \quad (18)$$

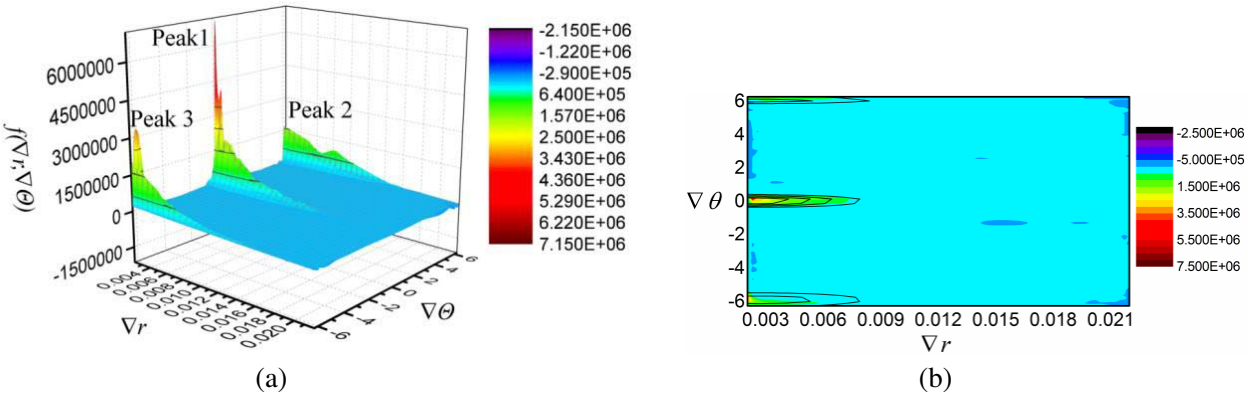

Figure 4. (a) Plot of integral function in two dimensional integration domain. (b) Contour plot of integral using Gaussian function by Levenberg Marquardt iteration algorithm.

Table 2. Parameters of fitted function.

Parameters	Peak1	Peak2	Peak3
t_0	7812.71	7812.71	7812.71
A	2.275E6	1.2439E6	1.079E6
r_c	0.00205	0.0025	0.0026
w_1	0.00324	0.00431	0.00386
s_c	0.02692	6.1	-5.9
w_2	0.19955	0.12763	0.29295

3. SOLUTION OF THE MULTIDIMENSIONAL FORCE INTEGRAL

The main objective of this work is to solve the four-dimensional complicated integral, given by Eq. (15). In most of the literatures, analytical or quasi-analytical solution of the elliptic integral is represented. In this paper, a numerical solution based on AMC integration technique is used to solve Eq. (15). At first, we search for the singularity and smoothness of the integrand. Then the adaptive sampling is done in the integration domain.

3.1. Adaptive Monte Carlo Integration

Standard available numerical integration techniques do not perform satisfactorily in multidimensional boundaries, particularly when the integrand is complicated and not smooth. Monte Carlo integration technique is very powerful in these circumstances, mostly for the problem involving integration which is too difficult to solve analytically and by other available numerical methods. Efficiency of Monte Carlo integration method increases relative to other methods when dimension of the integral increases. Other available methods, such as quadrature method become very complex and monotonous to solve in high dimension with complicated functions. Convergence of Monte Carlo method is guaranteed irrespective of problem dimension and smoothness of the function. Monte Carlo method is very simple and involves only two steps, random sampling integrand and point evaluation. Consider the problem of approximating the integral as shown in Eq. (19).

$$I = \int_{C^d} f(x)dx \tag{19}$$

where $x \in \Re^d$, $f(x)$ is the function of vector x, and C^d is the d-dimensional hyper rectangle $(a_1, b_1) \times (a_2, b_2) \ldots\ldots (a_d, b_d)$. In crude Monte Carlo (CMC), the integration is done by independently

sampling N points $\{x_i\}_{i=1}^{N}$ as per some suitable density function p and then the approximation of integral (Expectation E with respect to uniform distribution U in C^d) computing the estimate as shown in Eq. (20).

$$E^U f = \frac{C}{N} \sum_{i=1}^{N} \frac{f(x_i)}{p(x_i)} \tag{20}$$

where, $p(x_i)$ is the probability density function *pdf*. This estimated result is approximated and depends on where and how many samples are taken in the domain. If $p(x_i)$ is uniform probability density function and N is very large, then by the laws of large number the integration is given by Eq. (21).

$$I \cong E^U f = \frac{1}{N} \sum_{i=1}^{N} f(x_i) \tag{21}$$

In most of the practical problems, the integrand $f(x)$ varies significantly only in a small portion of overall integration domain C^d. The basic MC samples from a uniform distribution U waste calculation in the unimportant region. So a systematic procedure is required to allocate resources to the important region of the integration domain. In our proposed method, we use adaptive importance sampling, which discriminates important and non-important regions of the integration domain, as they progress. Variance of the sample average is given by Eq. (22)

$$V(f,p) = E^U \frac{f(x)^2}{p(x)} - \left(E^U f\right)^2 \tag{22}$$

When $p \equiv 1$, $V(f,p) \equiv V(f)$ with respect to uniform distribution U. The simple idea of importance sampling is to choose p such that $V(f,p) < V(f)$, and $p(x)$ is easy to sample and evaluate. In this work, an adaptive importance sampling (AIS) is considered where the sample density p is piecewise constant function and given by Eq. (23).

$$p = \sum_{k=1}^{K} p^k \chi_{\Omega^k}(x) \tag{23}$$

where Ω^k forms a partitioning of integration domain C^d into rectangular regions. $\chi_{\Omega^k}(x)$ is the characteristic function of Ω^k (1 if $x \in \Omega^k$ and 0 otherwise). The variance of the sample average can be written as Eq. (24).

$$V(f,p) = E^U \frac{f(x)^2}{p(x)} - (E^U f)^2 = \sum_{k=1}^{K} \frac{\int\limits_{\Omega^k} f(x)^2 dx}{p^k} - (E^U f)^2 \tag{24}$$

In AIS variance, $V(f,p)$ is minimized following the minimization problem in Eq. (25).

$$\begin{aligned} &\underset{\Omega^k,\, p^k}{\text{minimize}}\ V(f,p) = \sum_{k=1}^{K} \frac{\int\limits_{\Omega^k} f(x)^2 dx}{p^k} - \left(E^U f\right)^2 \\ &\text{Subjected to } \left\{\Omega^k\right\}_{k=1}^{K} \text{ is a partition of } C^d \\ &\sum_{k=1}^{K} p^k U(\Omega^k) = 1 \\ &p^k \geq 0 \ \forall\ k = 1 \ldots K \end{aligned} \tag{25}$$

If the partition $\{\Omega^k\}_{k=1}^{K}$ is fixed, then Eq. (25) becomes a convex optimization over weight p^k which can be solved by Lagrangian method. Lagrangian L is given by Eq. (26), and conditions for optimality

are given by Eqs. (27) and (28), respectively.

$$L(p,\lambda) = \sum_{k=1}^{K} \frac{\int_{\Omega^k} f(x)^2 dx}{p^k} - \left(E^U f\right)^2 + \lambda \left(\sum_{k=1}^{K} p^k U(\Omega^k) - 1 \right) \tag{26}$$

$$\partial_p L(p,\lambda) = 0 \tag{27}$$

$$\partial_\lambda L(p,\lambda) = 0 \tag{28}$$

Solving Eqs. (26)–(28), the optimal weight is given by Eq. (29)

$$p_0^k = \frac{\left(\frac{1}{U\Omega^k} \int_{\Omega^k} f(x)^2 dx \right)^{1/2}}{\sum_{k=1}^{K} \left(U\Omega^k \int_{\Omega^k} f(x)^2 dx \right)^{1/2}} \tag{29}$$

Optimal sampling density is given by Eq. (30).

$$p_0 = \sum_{k=1}^{K} p_0^k \chi_{\Omega^k} \tag{30}$$

Corresponding variance is given by Eq. (31).

$$\left(\sum_{k=1}^{K} \left(U\left(\Omega^k\right) \int_{\Omega^k} f(x)^2 dx \right)^{1/2} \right)^2 - \left(E^U f\right)^2 \tag{31}$$

AIS works recursively by partitioning C^d into rectangular subregions $[a^k, b^k]$ and splitting its elements in half along one of the co-ordinate axes. Let region Ω^k be partitioned into Ω^l, and it contributes to the variance through the term in Eq. (32).

$$\sum_{l} \left(U\left(\Omega^l\right) \int_{\Omega^l} f(x)^2 dx \right)^{1/2} \tag{32}$$

If we make partition $\{\Omega^l\}$ fine enough, it is possible to reduce the term in Eq. (27), and the optimal reduction of variance in Eq. (25) takes place. After a region is selected for partitioning, we have to decide along which of the d axis is to split. Let region $\{\Omega^k\}$ be divided into two subregions $\{\Omega^l\}$ and $\{\Omega^r\}$ due to a split along jth axis. The idea is that jth axis will be selected if the contribution towards the variance in Eq. (33) is minimum.

$$\left(U\left(\Omega^l\right) \int_{\Omega^l} f(x)^2 dx \right)^{1/2} + \left(U\left(\Omega^r\right) \int_{\Omega^r} f(x)^2 dx \right)^{1/2} \tag{33}$$

If f is similar about jth axis, there is no reduction in variance, and for that case, we have to split the region $\{\Omega^k\}$ into more than two subregions.

Algorithm

Step 1 Sample N points from the current density p^{it} in the iteration it.

Step 2 Compute the sample average $A_N(f, p^{it}) = \frac{1}{N} \sum_{i=1}^{N} \frac{f(x_i)}{p^{it}(x_i)}$ and estimate the variance $V_N(f, p^{it}) = \frac{1}{N-1} (\frac{1}{N} \sum_{=1}^{N} \frac{f(x_i)^2}{p^{it}(x_i)^2} - A_N(f, p^{it})^2)$.

Step 3 Compute the approximation $\tilde{m}_2^k = \frac{1}{U\Omega^k} \int\limits_{\Omega^k} f(x)^2 dx$ and $\tilde{m}_1^k = \frac{1}{U\Omega^k} \int\limits_{\Omega^k} f(x) dx$, refine the partitioning. Split the region, for which $U\Omega_k((\tilde{m}_2^k)^{1/2} - \tilde{m}_1^k)$ is greater than a certain constant ε^{it}.

Step 4 Set $p^{it+1} = (1-\varsigma) \sum\limits_{k=1}^{K} \tilde{p}_0^k \chi_{\Omega_k} + \varsigma$ where $\tilde{p}_0^k = \frac{(\tilde{m}_2^k)^{1/2}}{\sum\limits_{k=1}^{K} (U\Omega^k)(\tilde{m}_2^k)^{1/2}}$.

Where $\tilde{p}_0^k$ is the approximation of p_o for the current partition and $\varsigma \in (0,1)$. At the first iteration, only one hyper rectangle consists of the integration domain C^d. From the second iteration onwards, a rectangle is divided into two or more hyper rectangles unless stopping criteria are achieved.

Step 5 Compute the final sample average $A_N(f,p)$ which will give the integral approximation.

3.2. Smoothness of the Integrand

To have singularity, R_{Q1R1} must equal zero as per Eq. (14). So, the condition for singularity is given by Eq. (34).

$$(r_{OQ1}\cos\alpha - x - r_{O'R1}\cos\beta)^2 + (r_{OQ1}\sin\alpha - y - r_{O'R1}\sin\beta)^2 + (-z)^2 = 0 \tag{34}$$

Singularity exists if the distance between two elementary discretized magnetic surfaces $Q1$ and $R1$ becomes zero at plane $z = 0$. As shown in Figure 5, this distance never becomes zero as the inner magnet does not intersect the outer magnet at $z = 0$. Moreover, if we observe the surface plot of force $f(\nabla r, \nabla\theta)$ in Figure 3, it is evident that mainly three peaks constitute the surface, and all other portions in the domain is flat in nature and do not contribute too much towards the integration value. So the integrand force function does not have any kind of singularity.

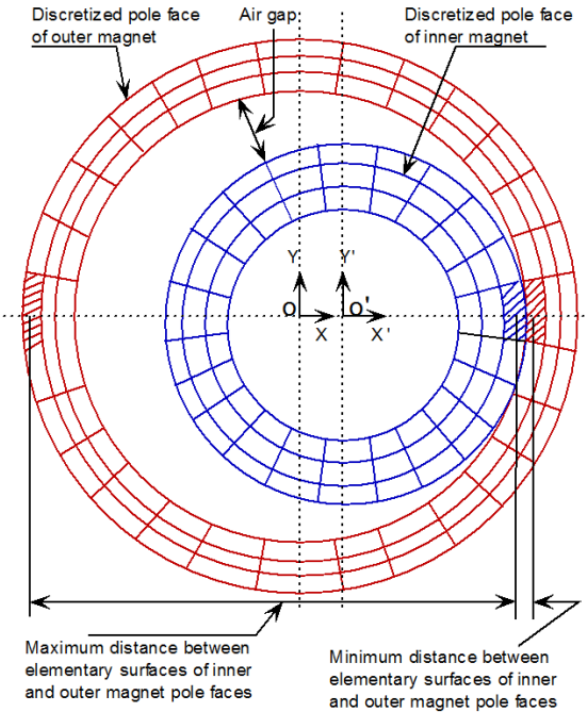

Figure 5. Maximum and minimum distances between discretized magnetic surfaces on inner and outer ring magnets respectively.

3.3. Importance Sampling

From Figure 4, it is observed that main contribution comes from the three peaks of the integrand function $f(\nabla r, \nabla\theta)$ in the integration domain, and all other portions are flat and have minor contribution towards

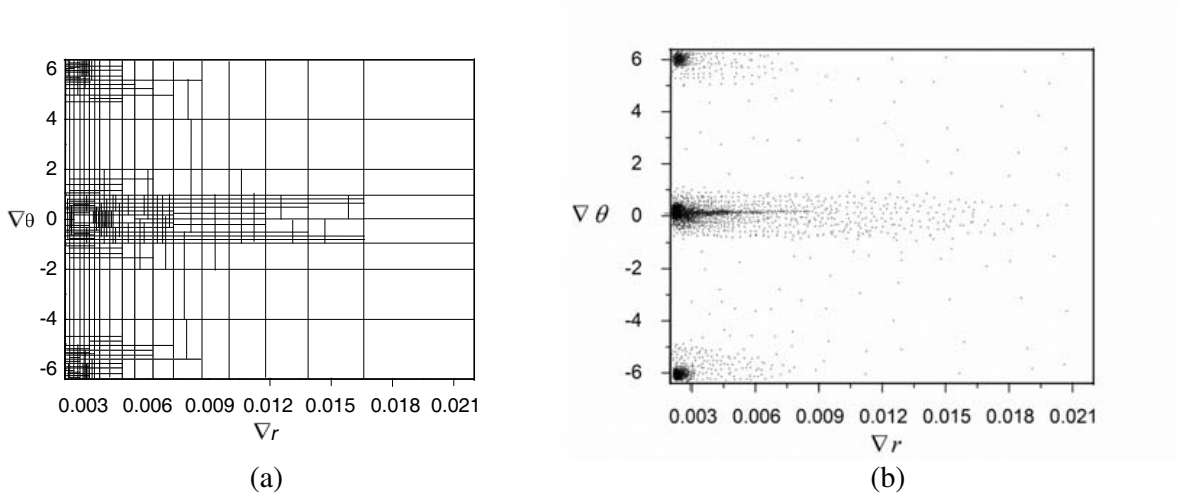

Figure 6. (a) Adaptive partining of integration domain by AMC. (b) Samples generated by Adaptive Importance Sampling (AIS).

the integration. So the flat distribution of sample points incurs error in the calculation unless numbers of random samples are very large. On the contrary, if number of sample is very large, computational cost will be high. Due to this irregular distribution of integrand, we consider adaptive distribution of sample points such that more samples are selected near peak and few samples in the flat region of integrand function in Figure 4. This is called importance sampling. As per the AMC algorithm, using the method discussed in Section 3.1, the adaptive partitioning of the integration domain is shown in Figure 6(a), and corresponding importance sampling is given by Figure 6(b). It is observed that more samples concentrate near the peaks, and few samples are in flat portion in the domain.

4. RESULT AND DISCUSSIONS

The practical magnetic configuration consists of two ring magnets, shown in Figure 7(a). Parameters of this magnetic system are given in Table 1. Our objective is to estimate the axial force between these two ring magnets for different positions of inner magnet. A laboratory test setup is fabricated to measure the axial force between two ring magnets, as shown in Figure 7(b). There is arrangement to

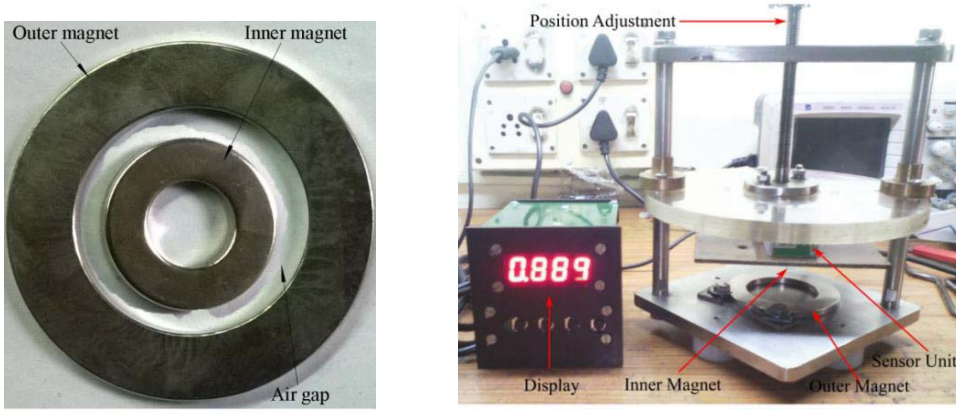

Figure 7. (a) Configuration of two ring magnets for laboratory testing. (b) Test set-up to measure force between two ring magnets.

Table 3. Output of algorithm upto third iterations for inner magnet displacement ($x = 0$, $y = 0$, $z = 2\,\text{mm}$).

Iteration no.	Partitions Ω_i^k	Estimated Integral	Estimated Error
0	Ω_0^1	173.153	0.251
	Ω	**173.153**	**0.251**
1	Ω_1^1	58.151	0.063
	Ω_1^2	114.213	0.142
	Ω	**172.364**	**0.155**
2	Ω_2^1	58.151	0.063
	Ω_2^2	72.432	0.081
	Ω_2^3	40.668	0.051
	Ω	**171.251**	**0.115**

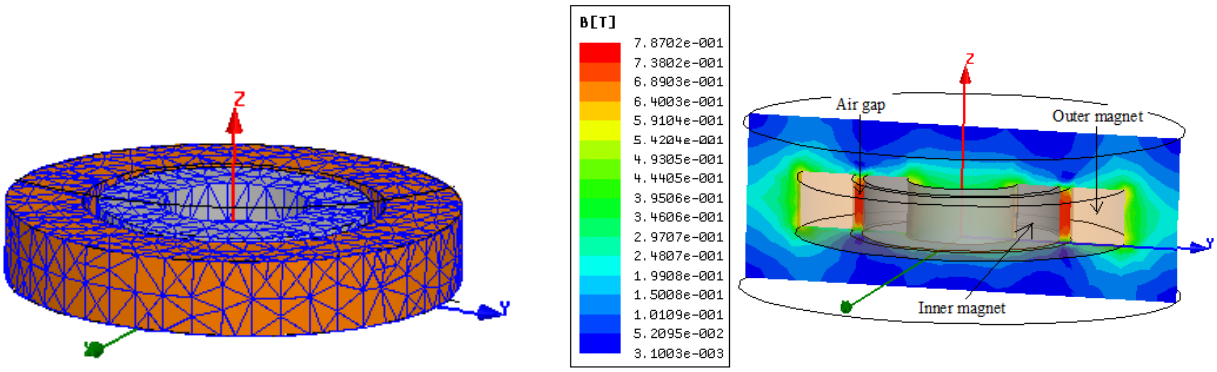

(a) (b)

Figure 8. (a) Mesh formation for FEM. (b) Flux density distribution for two ring magnets.

hold the two ring magnets. By a screw and nut arrangement, inner magnet can be placed at different axial positions, whereas the outer magnet is fixed. A sensor unit (load cell type) is used to measure the axial repulsive force between the two ring magnets, and a display is used to show the calibrated results. Once importance sampling is over, we estimate the sample average or the force integral between two ring magnets using method, discussed in Chapter 3.1. Table 3 shows the output of the AMC algorithm up to third iterations for inner magnet displacement $x = 0$, $y = 0$ and $z = 2\,\text{mm}$. We consider parameters $\varsigma = 0.01$ and $\varepsilon = 0.002$. It is observed that partitions are generated by dividing the region with maximum error. Figure 8(a) shows the mesh generated for FEM, and Figure 8(b) represents the magnetic flux density distribution in the air. Figure 9(a) shows the comparison of magnetic force, derived from three methods, AMC, FEM & [8]. We observe that results from these three methods are in close agreement with each other. Thus we validate the proposed AMC method by FEM and another established method by Ravaud [8]. Figure 9(b) represents the validation of AMC by experimental data. It is observed that if the self demagnetization is considered, AMC gives excellent results with respect to practical test results. In the course of execution, it is observed that computation time for AMC is 17 sec whereas FEM takes 34 sec. It is because AMC does not calculate for all the discrete magnetic surfaces, and it takes only importance sampling for prominent discrete surfaces which are very close to each others. Other methods such as FEM consider all the discrete magnetic surfaces on inner and outer magnet pole faces. Thus AMC also reduces the computation time.

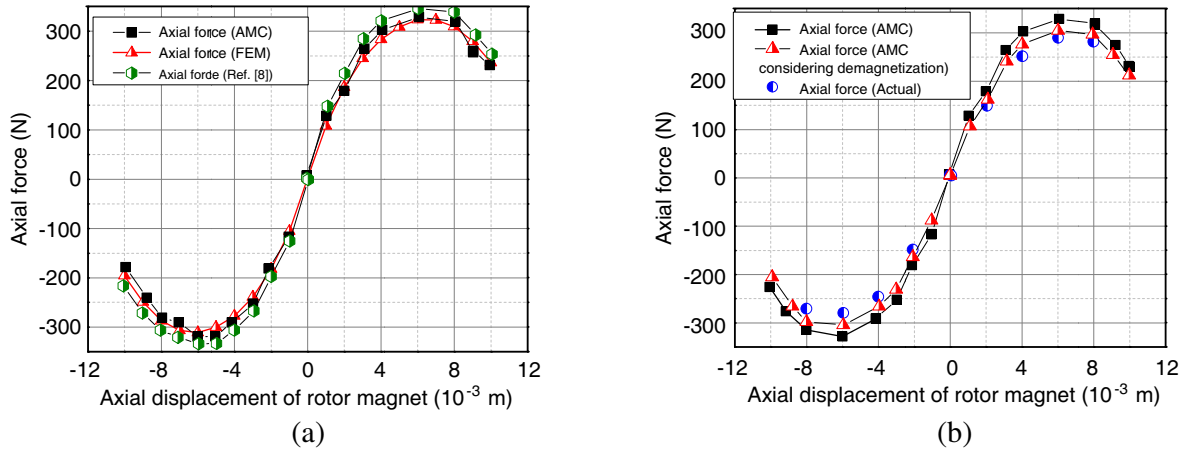

Figure 9. (a) Comparison of axial force computed by FEM, AMC and [8]. (b) Closeness of AMC results considering demagnetization with experimental results.

5. CONCLUSIONS

In this paper, a new technique is proposed to calculate magnetic force between two ring magnets using Adaptive Monte Carlo (AMC) integration. For higher dimension, this method is better fitted than conventional quadrature methods of integration. Equation of the force between two axially polarized ring magnets is developed using surface charge density method, and it incurs a four-dimensional integration. We investigate the singularity of the integrand function over the integration domain. It is observed that no singularity is possible as two ring magnets never intersect each other at horizontal plane. There are some peaks of integrand function in the domain which gives the main contribution to the integral. Due to these peaks, there is some error in the estimation. AMC also manages this problem very well just by choosing more random samples around the peak region than the flat portion of the integration domain. Finally, sample average is estimated which gives the integration value. Axial force between two ring magnets is evaluated using the proposed AMC method, FEM and Laboratory testing by shifting the inner magnet at different axial positions. These results are plotted, and a comparative study of the magnetic force is carried out. The results thus obtained are observed in good agreement with each other. This method is advantageous over existing analytical or quasi-analytical methods regarding singularity treatment and computational burden. It is more flexible, especially for using in digital computer. So taking into account of simplicity, less computational burden and usefulness, the proposed method may be an attractive alternative choice for magnetic force calculation.

ACKNOWLEDGMENT

This research work is sponsored by the Science and Engineering Research Board (SERB), order No. SR/S3/EECE/0164/2012, New Delhi, India.

REFERENCES

1. Chu, H. Y., Y. Fan, and C. S. Zhang, "A novel design for the flywheel energy storage system," *Proceedings of the Eighth International Conference on Electrical Machines and Systems*, Vol. 2, 1583–1587, 2005.
2. Ohji, T., et al., "Conveyance test by oscillation and rotation to a permanent magnet repulsive-type conveyor," *IEEE Trans. Magn.*, Vol. 40, No. 4, 3057–3059, 2004.
3. Hussein, A., et al., "Application of the repulsive-type magnetic bearing for manufacturing micro-mass measurement balance equipment," *IEEE Trans. Magn.*, Vol. 41, No. 10, 3802–3804, 2005.

4. Yonnet, J. P., "Passive magnetic bearings with permanent magnets," *IEEE Trans. Magn.*, Vol. 14, No. 5, 803–805, 1978.
5. Lang, M., "Fast calculation method for the forces and stiffness of permanent-magnet bearings," *8th International Symposium on Magnetic Bearing*, 533–537, 2002.
6. Jiang, W., et al., "Forces and moments in axially polarized radial permanent magnet bearings," *Proceedings of Eighth International Symposium on Magnetic Bearings*, 521–526, Mito, Japan, 2002.
7. Ravaud, R. and G. Lemarquand, "Comparison of the Coulombian and Amperian current models for calculating the magnetic field produced by radially magnetized arc-shaped permanent magnets," *Progress In Electromagnetics Research*, Vol. 95, 309–327, 2009.
8. Ravaud, R., G. Lemarquand, and V. Lemarquand, "Force and stiffness of passive magnetic bearings using permanent magnets. Part 1: Axial magnetization," *IEEE Trans. Magn.*, Vol. 45, No. 7, 2996–3002, 2009.
9. Ravaud, R., G. Lemarquand, V. Lemarquand, and C. Depollier, "Discussion about the analytical calculation of the magnetic field created by permanent magnets," *Progress In Electromagnetics Research B*, Vol. 11, 281–297, 2009.
10. Bekinal, S. I., A. R. Tumkur Ramakrishna, and S. Jana, "Analysis of axially magnetized permanent magnetic bearing characteristics," *Progress In Electromagnetic Research B*, Vol. 44, 327–343, 2012.
11. Lijesh, K. P. and H. Hirani, "Development of analytical equations for design and optimization of axially polarized radial passive magnetic bearing," *Journal of Tribology*, Vol. 137, 011103–9, 2015.
12. Mishra, M. and N. Gupta, "Monte Carlo integration technique for the analysis of electromagnetic scattering from conducting surfaces," *Progress In Electromagnetics Research*, Vol. 79, 91–106, 2008.
13. Pennanen, T. and M. Koivu, "An adaptive importance sampling technique," *Monte Carlo and Quasi-Monte Carlo Methods*, 443–455, Springer, 2004.
14. Alrefaei, M. H. and H. M. Abdul-Rahman, "An adaptive Monte Carlo integration algorithm with general division approach," *Math. Comput. Simul.*, 2007, doi:10.1016/j.matcom.2007.09.009.
15. Jourdain, B., "Adaptive variance reduction techniques in finance," *Radon Series Comp. Appl. Math.*, Vol. 8, 1–18, De Gruyter, 2009.
16. Parker, R. J., "Analytical methods for permanent magnet design," *Electro-Technology*, 1960.